

Efficiency of lidar operation through a localized layer of a scattering medium

A.N. Glushkov and A.L. Mitrofanov

The Fifth Central Scientific Research Experiments Institute, Voronezh

Received October 18, 1999

The efficiency of operation of a lidar system with coherent and incoherent information processing through a localized scattering layer has been theoretically studied, and an engineering technique for its estimation has been developed.

Introduction

The study of the influence the medium of beam propagation on the efficiency of operation of a lidar system is an urgent problem, because in most cases it is just the medium that determines the potential capabilities of lidars in detecting objects and measuring their parameters.¹ In Refs. 1–3 the influence of scattering layers on the structure and power of a return signal was considered. The problem was solved by the methods of photometry as applied to sensing of an unlimited Lambertian surface.

The results obtained may be useful in analyzing the quality of lidar systems with incoherent processing of a received signal. The applicability of lidar systems depends on the type of the surface sounded, as well as on the ratio between its size and the beam cross section. However, there is a drawback in the approach developed to process lidar returns that, first, it does not allow for the diffraction effects accompanying propagation and scattering of laser radiation and, second, it is inapplicable to analysis of the influence of scattering media on the operation of lidar systems with coherent processing of the received signals. These drawbacks can be overcome by using numerical methods.^{3,4} However, they are very computationally expensive, so that the influence of scattering media on the characteristics of lidar systems that use different modes of the received signal processing cannot be estimated on the real-time scale.

This paper was primarily aimed at developing an engineering technique for estimating the influence of a localized scattering layer on the efficiency of lidar systems that use direct detection and heterodyning of the received signals.

1. Technique for estimating the efficiency of lidar systems

The geometry of the lidar problem under consideration is shown in Fig. 1, where *A* is the plane of the lidar system; *B* is the plane of entrance to the localized scattering layer; *C* is the plane of exit from the scattering layer; *D* is the object plane; $\mathbf{r}_1, \mathbf{r}_2; \boldsymbol{\eta}_1, \boldsymbol{\eta}_2; \mathbf{q}_1, \mathbf{q}_2; \mathbf{s}_1, \mathbf{s}_2$ are the radius vectors describing positions of the points in the planes *A*, *B*, *C* and *D*, respectively; $\mathbf{R}, \boldsymbol{\rho}; \boldsymbol{\eta}, \boldsymbol{\omega}; \mathbf{V}, \mathbf{q}; \mathbf{S}, \mathbf{p}$ are the sum and

difference radius vectors in the corresponding planes; \mathbf{b} is the unit vector along the direction of scattering; \mathbf{b}' is the unit vector of the radiation incident on an elementary scatterer.

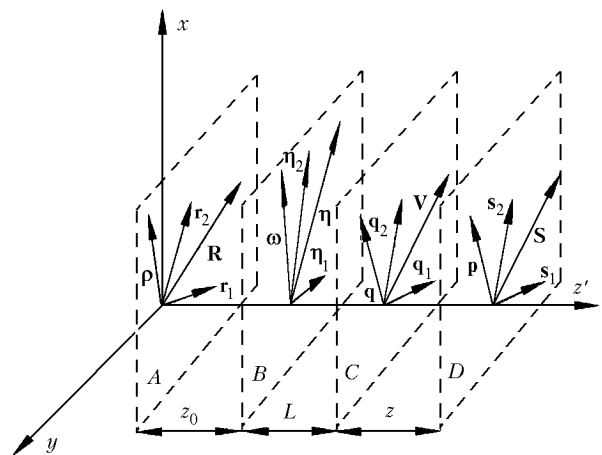


Fig. 1. The geometry of the lidar problem.

The main parameter determining the detection limit and the limiting accuracy of lidar systems in obtaining coordinates and other information on remote objects is the signal-to-noise ratio at the output of a postdetector filter of a lidar recording unit.^{5–7} This ratio can be written as follows:

$$Q_\chi = \langle |j_s^\chi(t)|^2 \rangle / \langle |j_n^\chi(t)|^2 \rangle,$$

where $\langle |j_s^\chi(t)|^2 \rangle$ and $\langle |j_n^\chi(t)|^2 \rangle$ are the mean squares of the signal and noise components of the radiant flux. These are determined as follows^{5,7}:

$$\langle |j_s^c(t)|^2 \rangle = \left(\frac{\beta e}{\hbar \nu} \right)^2 \times \int \int_{\Sigma} \Gamma_{2s}(\mathbf{r}_1, \mathbf{r}_2, \tau) \Gamma_{2h}(\mathbf{r}_1, \mathbf{r}_2) T(\mathbf{r}_1, \mathbf{r}_2) d^2\mathbf{r}_1 d^2\mathbf{r}_2; \quad (1)$$

$$\langle |j_n^c(t)|^2 \rangle = \left[\frac{\beta e}{\hbar \nu} \int_{\Sigma} \Gamma_{2h}(\mathbf{r}_1, \mathbf{r}_2 = 0) T(\mathbf{r}_1, \mathbf{r}_2 = 0) d^2\mathbf{r}_1 \right] e \Delta f; \quad (2)$$

$$\langle |j_n^{inc}(t)|^2 \rangle = \frac{\beta e}{\hbar \nu} [N_b \Delta \nu + 2\hbar \nu \langle |j_c^{inc}(t)|^2 \rangle] \times \sqrt{\Delta f} / \beta e + P_{bsn}(t) \sqrt{\Delta f} e; \quad (3)$$

$$\langle |j_s^{\text{inc}}(t)|^2 \rangle = \frac{\beta e}{\hbar \nu} \int_{\Sigma} \Gamma_{2h}(\mathbf{r}_1, \mathbf{r}_2=0) T(\mathbf{r}_1, \mathbf{r}_2=0) d^2\mathbf{r}_1, \quad (4)$$

where β is the quantum efficiency of the photodetector; e is the electron charge; \hbar is the Planck's constant; ν is the laser radiation frequency; Σ is the area of the receiving aperture; $\Gamma_{2s}(\mathbf{r}_1, \mathbf{r}_2, \tau)$ is the second-order function of coherence (FC) of the optical lidar return; $\Gamma_{2h}(\mathbf{r}_1, \mathbf{r}_2)$ is the FC of radiation from the local oscillator; $T(\mathbf{r}_1, \mathbf{r}_2)$ is the transmission of the optical receiving channel of the lidar; N_b is the spectral power density of the background radiation; $P_{\text{bsn}}(t)$ is the backscattering noise power; $\Delta\nu$ is the pass band of the lidar receiving system; Δf is the pass band of the postdetector filter; τ is the time lag; χ is the subscript equal to "inc" for lidar systems with a direct detector (incoherent lidar systems) and "c" for a heterodyne lidar system (coherent lidar system).

From Eqs. (1)–(4) it is seen that to find the sought parameters Q_χ , we should first find the FC of the lidar return signal in the plane of the receiving aperture of the lidar system.

The FC of the return signal can be found as^{1,2}:

$$\begin{aligned} \Gamma_{2s}(\mathbf{r}_1, \mathbf{r}_2, \tau) &= \Gamma_{2s}(\mathbf{R}, \boldsymbol{\rho}, \tau) = \int \dots \int \Gamma_{2p}(\mathbf{R}', \boldsymbol{\rho}', \tau) \times \\ &\times G_{AB}(\mathbf{R}', \boldsymbol{\rho}', \boldsymbol{\eta}', \boldsymbol{\omega}) \hat{G}_{BC}(\boldsymbol{\eta}', \boldsymbol{\omega}'; \mathbf{V}', \mathbf{q}') \times \\ &\times G_{CD}(\mathbf{V}', \mathbf{q}', \mathbf{S}, \mathbf{p}) U(\mathbf{S}, \mathbf{p}) G_{CD}^*(\mathbf{S}, \mathbf{p}; \mathbf{V}, \mathbf{q}) \times \\ &\times \hat{G}_{BC}^*(\mathbf{V}, \mathbf{q}; \boldsymbol{\eta}, \boldsymbol{\omega}) G_{AB}^*(\boldsymbol{\eta}, \boldsymbol{\omega}; \mathbf{R}, \boldsymbol{\rho}) d^2R' d^2\rho' d^2\eta' \leftrightarrow \\ &\leftrightarrow d^2\omega' d^2V' d^2q' d^2S d^2p d^2V d^2q d^2\eta d^2\omega, \quad (5) \end{aligned}$$

where $\Gamma_{2p}(\bullet)$ is the FC of the sounding radiation; $U(\bullet)$ is the function describing the reflection characteristics of the object; $G_{AB}(\bullet)$ and $G_{CD}(\bullet)$ are the Green's functions of the paths "lidar – scattering layer" and "scattering layer – object," respectively; $\hat{G}_{BC}(\bullet)$ is the transfer function of the scattering layer; the asterisk denotes complex conjugation.

The transfer function of the scattering layer can be found by solving the transfer equation⁹ in the form

$$\begin{aligned} \hat{G}_{BC}(\boldsymbol{\eta}, \boldsymbol{\omega}; \mathbf{V}, \mathbf{q}) &= \left(\frac{K}{2\pi L} \right)^2 \exp \left\{ i \frac{K}{L} (\mathbf{V} - \boldsymbol{\eta}) (\mathbf{q} - \boldsymbol{\omega}) - \right. \\ &\left. - \alpha_t + \frac{1}{4\pi} \int_0^L d\zeta P \left[k\boldsymbol{\omega} + \frac{\zeta}{L} K(\mathbf{q} - \boldsymbol{\omega}) \right] \right\}, \end{aligned}$$

where

$$\begin{aligned} P(\boldsymbol{\xi}) &= \iint p(\mathbf{b}) \exp \{ i\mathbf{b} \boldsymbol{\xi} \} d^2b; \\ K &= \text{Re} \{ k + 2\pi f_{\text{sc}}(\mathbf{b}, \mathbf{b}') \rho_{\text{sc}} / k \}; \end{aligned}$$

$k = 2\pi/\lambda$; λ is the wavelength of sounding radiation; $\alpha_t = \rho_{\text{sc}} \sigma_t L$ is the total extinction coefficient (optical density of the local layer); ρ_{sc} is the density of scatterers; $\sigma_t = \sigma_a + \sigma_{\text{sc}}$ is the total extinction cross section, σ_a is the absorption cross section, σ_{sc} is the

scattering cross section; $p(\bullet) = \frac{4\pi}{\sigma_t} |f_{\text{sc}}(\mathbf{b}, \mathbf{b}')|^2$, $f_{\text{sc}}(\mathbf{b}, \mathbf{b}')$ is the scattering phase function of an elementary scatterer.

For spherical scatterers, taking into account that $p(\mathbf{b}, \mathbf{b}') \approx \frac{\alpha \sigma_{\text{sc}}}{\pi \sigma_t} \exp \{-\alpha \theta^2\}$ (Ref. 8), the function $\hat{G}_{BC}(\bullet)$ can be found as:

$$\begin{aligned} \hat{G}_{BC}(\boldsymbol{\eta}, \boldsymbol{\omega}; \mathbf{V}, \mathbf{q}) &= \left(\frac{k}{2\pi L} \right)^2 \exp \left\{ i \frac{k}{L} (\mathbf{V} - \boldsymbol{\eta}) (\mathbf{q} - \boldsymbol{\omega}) - \alpha_t + \right. \\ &\left. + \rho_{\text{sc}} \sigma_{\text{sc}} \int_0^L d\zeta \exp \left\{ - \frac{[\boldsymbol{\omega} - \boldsymbol{\xi}/L (\mathbf{q} - \boldsymbol{\omega})]^2}{4s^2} \right\} \right\}, \quad (6) \end{aligned}$$

where θ is the angle between the vectors \mathbf{b} and \mathbf{b}' ; $\alpha \approx 2.66 (d/\lambda)^2$; d is the scatterer diameter ($d \gg \lambda$); $\sigma_{\text{sc}} \approx 2\pi(d/2)^2$, $s^2 \approx 10.64 d^2/\pi$.

To derive, in an explicit form, analytical equations for Q_c and Q_{inc} , let us make use of the following approximation of the transfer function of the scattering layer:

$$\begin{aligned} \hat{G}_{BC}(\boldsymbol{\eta}, \boldsymbol{\omega}; \mathbf{V}, \mathbf{q}) &= \left(\frac{k}{2\pi L} \right)^2 \exp \left\{ i \frac{k}{L} (\mathbf{V} - \boldsymbol{\eta}) (\mathbf{q} - \boldsymbol{\omega}) - \alpha_t \right\} \times \\ &\times \sum_{n=0}^{\infty} \frac{(\alpha_{\text{sc}})^n}{n!} \exp \left\{ -n \frac{(\mathbf{q} - \boldsymbol{\omega})^2}{4s^2} \right\}, \quad (7) \end{aligned}$$

and determine the functions $\Gamma_{2p}(\bullet)$, $G_{AB}(\bullet)$, and $T(\bullet)$ by the Gauss models proposed in Refs. 1 and 2.

The noise power of backscattering from the local layer for the monostatic coaxial sensing scheme, by analogy with Ref. 2, can be found from the following equation:

$$\begin{aligned} P_{\text{bsn}}(t) &= \int_{z_0}^{z_0+L} d\zeta \int d\boldsymbol{\eta} \sigma_{\text{sc}}(\zeta) f_{\text{sc}}(\boldsymbol{\eta}, \zeta) T_a^2 \times \\ &\times \Gamma_{2p}(z_0, \boldsymbol{\eta}, 0, 0) \Gamma_{2r}(z_0 + L, \boldsymbol{\eta}, 0, 0) f^2(t - 2\zeta/c), \quad (8) \end{aligned}$$

where $f_{\text{sc}}(\boldsymbol{\eta}, z)$ is the backscattering phase function; $T_a = \exp \{-\alpha_t L\}$; $\Gamma_{2r}(z_0 + L, \boldsymbol{\eta}, \boldsymbol{\omega}) = \int T(\mathbf{R}, 0) \times G_{AB}(\mathbf{R}, \boldsymbol{\rho}; \boldsymbol{\eta}, \boldsymbol{\omega}) d^2R$; $f(t)$ is the envelope of the sensing pulse; c is the speed of light.

Equation (8) with regard for the accepted models, as well as the fact that

$$f(t) = 2/\sqrt{\pi} \exp \{-4t^2/\tau_p^2\},$$

where τ_p is the sensing pulse duration, takes the form

$$\begin{aligned} P_{\text{bsn}}(t) &= U_0^2 \frac{\pi a_{\text{tr}}^2 \sigma_{\text{sc}} \rho_{\text{sc}} f_{\text{sc}}(\boldsymbol{\eta}) T_a^2 a_{\text{tr}}^2 \tau_p c}{1 + a_{\text{tr}}^2/a_e^2} \frac{1}{a_e^2 \sqrt{\pi}} \times \\ &\times \left[\text{erf} \left(\frac{2(z_0 + L)}{c\tau_p} + \frac{t}{\tau_p} \right) - \text{erf} \left(\frac{2z_0}{c\tau_p} + \frac{t}{\tau_p} \right) \right], \end{aligned}$$

where a_e is the effective radius of the sensing beam at the entrance to the layer; $\text{erf}(\bullet)$ is the error function.¹⁰

It is convenient to analyze the influence of a localized scattering layer on the characteristics of a lidar system by the relative indices $\tilde{\mu}_{inc}$ and $\tilde{\mu}_c$ normalized to $\exp\{-2\alpha_a L\}$ (α_a is the absorption coefficient):

$$\tilde{\mu}_{inc} = \frac{Q_{inc}^a}{Q_{inc}^0} = \frac{P_{inc}^a / Q_{inc}^0}{P_{inc}^0 / Q_{inc}^0 + P_{bsn} / P_{inc}^a} \exp\{2\alpha_{ii} L\};$$

$$\tilde{\mu}_c = \frac{Q_c^a}{Q_c^0} = \frac{P_c^a}{P_c^0} \exp\{2\alpha_a L\},$$

where Q_{ins}^a , Q_{ins}^0 , Q_c^a , Q_c^0 and P_{inc}^a , P_{inc}^0 , P_c^a , P_c^0 are respectively the signal-to-noise ratios and powers of the return signal at the coherent and incoherent processing in the presence (“a”) and absence (“0”) of the scattering layer.

Table 1

No.	Object model	Efficiency of lidar system with incoherent signal processing	Efficiency of lidar system with coherent signal processing
1	Point-like reflector $U(\mathbf{r}) = 2\pi \frac{V_t}{k^2} \delta(\mathbf{r})$	$\mu_{inc} = \frac{\sum_{n,m=0}^{\infty} \frac{\alpha_{sc}^n}{n!} \frac{\alpha_{sc}^m}{m!} a_{ev}^{-2} \frac{\Omega_z^2}{\Omega_e^2} v_5^{-1}}{a_{ev0}^{-2} \frac{\Omega_{z0}^2}{\Omega_{e0}^2} v_{50}^{-1}} \Psi_1 T_a^2$	$\mu_c = \frac{\sum_{n,m=0}^{\infty} a_{es}^{-2} a_{esr}^{-2} \frac{\alpha_{sc}^n}{n!} \frac{\alpha_{sc}^m}{m!}}{a_{es0}^{-2} a_{esr0}^{-2}} T_a^2$
2	Diffuse object $U(\mathbf{r}_1, \mathbf{r}_2) = \frac{4\pi}{k^2} V_d^2 \times \exp\left\{-\frac{r_1^2 + r_2^2}{2a_d^2}\right\} \times \delta(\mathbf{r}_1 - \mathbf{r}_2)$	$\mu_{inc} = \frac{\sum_{n,m=0}^{\infty} \frac{\alpha_{sc}^n}{n!} \frac{\alpha_{sc}^m}{m!} \left(1 + a_{ev}^2 \frac{\Omega_e^2}{\Omega_z^2} \frac{v_5}{a_d}\right)^{-1}}{\left(1 + a_{ev0}^2 \frac{\Omega_{e0}^2}{\Omega_{z0}^2} \frac{v_{50}}{a_d}\right)^{-1}} \Psi_2 T_a^2$	$\mu_c = \frac{\sum_{n,m=0}^{\infty} a_{esr}^{-2} \frac{\alpha_{sc}^n}{n!} \frac{\alpha_{sc}^m}{m!} \left(1 + \frac{a_{es}^2}{a_d^2} + \frac{a_{es}^2}{a_{esr}^2}\right)^{-1}}{a_{esr0}^{-2} \left(1 + \frac{a_{es0}^2}{a_d^2} + \frac{a_{es0}^2}{a_{esr0}^2}\right)^{-1}} T_a^2$
3	Specular reflector $U(\mathbf{r}) = V_{sr} \exp\left\{-\frac{r^2}{2a_{sr}^2}\right\} \times \delta(\mathbf{r} - \mathbf{r}_r)$	$\mu_{inc} = \frac{\sum_{n,m=0}^{\infty} \frac{\alpha_{sc}^n}{n!} \frac{\alpha_{sc}^m}{m!} a_{ev}^2 v_9^{-1} v_{10}^{-1}}{a_{ev0}^2 v_{90}^{-1} v_{100}^{-1}} \Psi_3 T_a^2$	$\mu_c = \frac{\sum_{n,m=0}^{\infty} \frac{\alpha_{sc}^n}{n!} \frac{\alpha_{sc}^m}{m!} \frac{a_{esr}}{a_c^2} v_7^{-1} v_8^{-1}}{\frac{a_{esr0}^2}{a_{ec0}^2} v_{70}^{-1} v_{80}^{-1}} T_a^2$

Note. Index “0” means the absence of local scattering layer.

In Table the following designations are used:

$$v_{10} = \Omega_z^2 \frac{v_4}{v_5} + \frac{mL^2 a_{ev}^2}{s^2(z_0 + z + L)^2} + \frac{k^2 a_r^2 r_2^2}{(z_0 + z + L)^2} + \Omega_e^2 \frac{v_5}{v_9} \left(\frac{v_6}{v_5} + \Omega_z^{-1} \frac{ka_{ev}^2}{(z_0 + z + L)^2} \right)^2, \quad v_9 = \left(1 + \frac{a_{ev}^2 v_5 \Omega_e^2}{a_{sr}^2 \Omega_z^2} \right),$$

$$v_8 = 1 + \frac{a_{ec}^2}{a_{sr}^2} + \frac{a_{ec}^2}{a_{ecr}^2} + \left[v_e + v_{er} \frac{a_{es}^2}{a_{esr}^2} \right]^2 \frac{a_{ec}^2}{a_{es}^2} v_7^{-1}, \quad v_7 = 1 + \frac{a_{es}^2}{a_{sr}^2} + \frac{a_{es}^2}{a_{esr}^2},$$

$$v_6 = v_4 + v_3 (v_3 + \Omega_z / \Omega_e), \quad v_{6r} = v_{4r} + v_{3r} (v_{3r} + \Omega_{zr} / \Omega_{er}), \quad v_5 = v_4 + (v_3 + \Omega_z / \Omega_e)^2, \quad v_{5r} = v_{4r} + (v_{3r} + \Omega_{zr} / \Omega_{er})^2,$$

$$v_4 = v_2 + n (a_{ev}^2 / s^2) \Omega_e^{-2}, \quad v_{4r} = v_{2r} + m (a_{evr}^2 / s^2) \Omega_{er}^{-2},$$

$$v_3 = (1 + \gamma / \Omega_e) \gamma \Omega_e^{-1} + (a_e^2 / \rho_a^2) \Omega_e^{-2}, \quad v_{3r} = (1 + \gamma_r / \Omega_{er}) \gamma_r \Omega_{er}^{-1} + (a_{er}^2 / \rho_{ar}^2) \Omega_{er}^{-2},$$

$$v_2 = \Omega_e^{-2} \{ (a_e^2 / \rho_a^2) + n (a_e^2 / s^2) [1 - 2\gamma \Omega_e^{-1} - n (a_e^2 / s^2) \Omega_e^{-2}] \}, \quad v_{2r} = \Omega_{er}^{-2} \{ (a_{er}^2 / \rho_{ar}^2) + m (a_{er}^2 / s^2) [1 - 2\gamma_r \Omega_{er}^{-1} - m (a_{er}^2 / s^2) \Omega_{er}^{-2}] \},$$

$$v_1 = (1 - \gamma / \Omega_e)^2 + (a_e^2 / \rho_a^2) \Omega_e^{-2} + n (a_e^2 / s^2) \Omega_e^{-2}, \quad v_{1r} = (1 - \gamma_r / \Omega_{er})^2 + (a_{er}^2 / \rho_{ar}^2) \Omega_{er}^{-2} + m (a_{er}^2 / s^2) \Omega_{er}^{-2};$$

$$\Omega_e = ka_e^2 / L, \quad \Omega_z = ka_{ev}^2 / z, \quad \Omega_{er} = ka_{evr}^2 / L; \quad \Omega_z = ka_{evr}^2 / z; \quad a_{ev}^2 = a_e^2 v_1; \quad a_{evr}^2 = a_{er}^2 v_{1r},$$

$$a_e^2 = a_{tr}^2 [1 + \Omega_{tr}^{-2} (1 + a_{tr}^2 / a_c^2)], \quad a_{er}^2 = a_r^2 + \Omega_r^{-2} a_r^2;$$

$$\rho_a^2 = a_e^2 [1 + a_{tr}^2 / a_c^2]; \quad \gamma = \Omega_{tr}^{-1} (1 + a_{tr}^2 / a_c^2); \quad \rho_{ar}^2 = a_{er}^2; \quad \gamma_r = \Omega_r^{-1};$$

$$\Omega_{tr} = \frac{k a_{tr}^2}{z_0}; \quad a_{es}^2 = \frac{a_{ev}^2 v_5 \Omega_e^2}{\Omega_z^2}; \quad \Omega_r = \frac{k a_r^2}{z_0}; \quad a_{esr}^2 = \frac{a_{evr}^2 v_{5r} \Omega_{er}^2}{\Omega_{zr}^2}; \quad a_e^2 = \frac{a_{ev}^2 v_5}{\Omega_z^2 v_4}; \quad v_e = \frac{\Omega_e^2 v_6}{\Omega_z}; \quad a_{esr}^2 = \frac{a_{evr}^2 v_{5r}}{\Omega_z^2 v_{4r}}; \quad v_{er} = \frac{\Omega_{er}^2 v_{6r}}{\Omega_{zr}};$$

$$\Psi_1 = \frac{1 / Q_{inc}^0}{1 / Q_{inc}^0 + \frac{V_t^2 \Omega_{z0}^2 (1 + a_r^2 / a_{e0}^2) a_{e0}^2 \sqrt{\pi}}{(2\pi)^4 (z_0 + z + L)^2 k^2 a_{ev0}^2 \Omega_{e0}^2 v_{50} \sigma_{sc} \rho_{sc} f_{sc}(\pi) c \tau_p} E}, \quad \Psi_2 = \frac{1 / Q_{inc}^0}{1 / Q_{inc}^0 + \frac{V_d^2 (1 + a_r^2 / a_{e0}^2) v_9^{-1} a_e^2}{(2\pi)^4 (z_0 + z + L)^2 \sigma_{sc} \rho_{sc} f_{sc}(\pi) c \tau_p} E};$$

$$\Psi_3 = \frac{1 / Q_{inc}^0}{1 / Q_{inc}^0 + \frac{V_{sr}^2 (1 + a_r^2 / a_{e0}^2) v_9^{-1} v_{10}^{-1} a_e^2 a_{ev}^2}{\pi \lambda^2 (z_0 + z + L)^2 \sigma_{sc} \rho_{sc} f_{sc}(\pi) c \tau_p} E}; \quad E = \operatorname{erf}\left(\frac{2(z_0 + L)}{c \tau_p} + \frac{t_1}{\tau_p}\right) - \operatorname{erf}\left(\frac{2z_0}{c \tau_p} + \frac{t_1}{\tau_p}\right);$$

a_{tr} is the effective radius of the lidar transmitter; a_c is the coherence length of sensing radiation; n and m are summation indices. Calculations were made for a collimated beam.

The calculated results are given in Table 1. The reflection characteristics of the object sounded were set in accordance with the known models of point-like, specular, and diffuse reflectors.^{1,5} In calculations, t was the time of arrival of the return pulse reflected from the target. This time is calculated as $t = 2(z_0 + L + z)/c$.

The obtained equations allow us to analyze the influence of localized layers of scattering media on the efficiency of lidar systems with coherent and incoherent signal processing from a unified theoretical basis. Besides, they allow us to take into account the main parameters of lidar transmitting-receiving systems, scattering properties of objects, and diffraction effects accompanying formation and propagation of lidar signals. It is interesting to compare the results obtained by the developed technique with the known results on the influence of scattering layers on the characteristics of lidar returns. Figure 2 shows the calculated results on the normalized power of the signal backscattered from a diffuse surface and received by a detector.

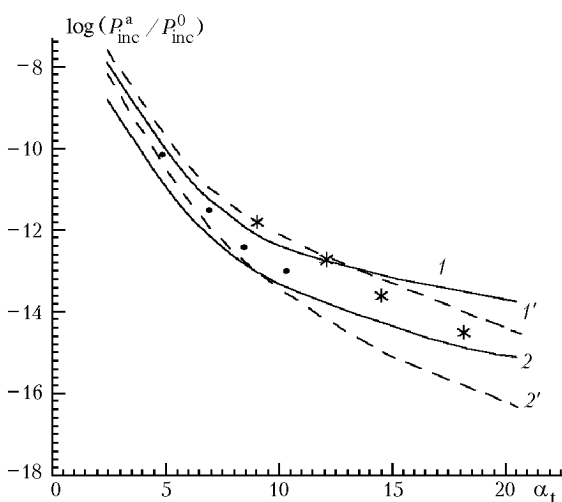


Fig. 2. Normalized power of received signal vs. distance between transmitter and diffuse surface: calculation by the proposed technique (1 and 2); results of Ref. 2 (1' and 2'); experimental data of Ref. 11 (ω and \bullet). Initial data for 1, 1', and ω : $\varphi_{tr} \alpha_t = 2.8 \cdot 10^{-3}$; $\varphi_r \alpha_t = 1.9 \cdot 10^{-2}$; $\alpha_{sc}/\alpha_t = 0.8$; and for 2, 2', and \bullet : $\varphi_{tr} \alpha_t = 1.6 \cdot 10^{-3}$; $\varphi_r \alpha_t = 1.0 \cdot 10^{-2}$; $\alpha_{sc}/\alpha_t = 0.78$; (φ_{tr} and φ_r are the angular dimensions of radiation transmitter and receiver, respectively).

Dependences 1 and 2 were calculated by the developed technique; dependences 1' and 2' and the experimental results were obtained in Refs. 2 and 11. The initial data, for which these dependences were obtained, are given in the figure caption. The results presented allow the conclusion that the developed technique gives dependences, which are in close qualitative and satisfactory quantitative agreement with the results known from literature. The quantitative difference between the plots 1, 2 and 1', 2' can be explained as follows. The plots 1' and 2' were obtained

in Ref. 2 with the use of the diffusion version of the small-angle approximation. In this approximation the scattering phase function is assumed isotropic at small scattering angles.

The developed technique is based on the theory of scattering by spherical particles of large diameter. It should be noted that in this case the identity of sizes of all particles does not restrict the generality of the equations obtained, since the case of different-size particles can be taken into account by averaging over particle size.⁹ Analysis we have performed allows to draw a conclusion that the developed technique can be used for obtaining engineering estimates of the influence of localized scattering layers on the efficiency of operation of a lidar system with coherent and incoherent signal processing.

2. Results of estimation of lidar system efficiency

The efficiencies μ_{inc} and μ_c were estimated for the case of sensing point-like, specularly reflecting, and diffuse reflectors depending on the characteristics of the scattering layer and diffraction parameters of the transmitting-receiving system of a lidar. The obtained results are shown in Figs. 3–9.

Figures 3–5, 7, and 8 show the dependence of the lidar operation efficiency on the position of a scattering layer. It is seen from the figures that when sensing point-like and diffuse objects, as well as a specularly reflecting one with a coherent lidar system, the “tracing-paper” effect is manifested quite distinctly,¹² i.e., the closer is the layer to the object, the less is the influence of the layer on μ_χ . For an incoherent lidar system, the less is the aperture of the lidar receiver and the less is the geometric thickness of the optical layer at fixed density, the more pronounced is this effect. When sensing a specularly reflecting object, the “tracing-paper” effect manifests itself if the scattering layer is nearby the lidar. It is also seen from the obtained results that the larger is the ratio d/λ , the stronger is the influence of the scattering layer on the efficiency of an incoherent lidar system. At $d/\lambda \geq 10$ the dependence $\mu_{inc} = f(d/\lambda)$ saturates.

The nature of these effects is in the growth of the contribution coming from radiation scattered outside the layer as the layer thickness and the ratio d/λ decrease. The tendency of the efficiency of an incoherent lidar system, as a function of d/λ , to saturate is explained by the fact that the scattering cross section of a particle at large values of the Mie parameter tends to its limiting value.¹³ In this case, no matter what the type of an object, the “tracing-paper” effect manifests itself if the scattering layer is near the object. This result follows from the Van Zittert–Zernike theorem¹³: the degree of coherence of a lidar signal increases with the increasing distance from the secondary source of radiation.

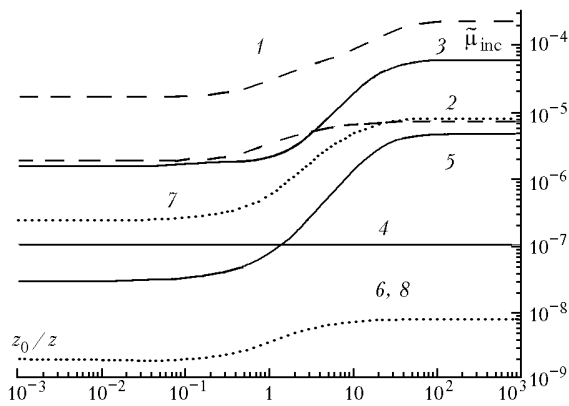


Fig. 3. Dependence of $\tilde{\mu}_{inc}$ on the position of a scattering layer when sensing a diffusely reflecting object and at $a_{tr}/a_c = 0$, $R/F = 0$, $d/\lambda = 3$ (1–6), $d/\lambda = 1$ (7, 8), $a_{tr}/a_r = 1$ (1, 2, 5, 6, 7, 8), $a_{tr}/a_r = 0.1$ (3, 4), $\alpha_{sc} = 1.41$ (1–8), $L = 10$ m (1, 3, 5, 7), $L = 100$ m (2, 4, 6, 8).

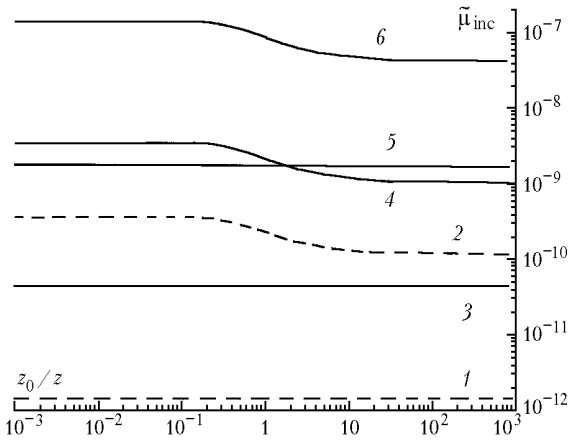


Fig. 4. Dependence of $\tilde{\mu}_{inc}$ on the position of a scattering layer when sensing a specularly reflecting object and at $a_{tr}/a_c = 0$, $R/F = 0$, $d/\lambda = 1$ (1, 2), $d/\lambda = 3$ (3, 4, 5, 6), $a_{tr}/a_r = 1$ (1, 2), $a_{tr}/a_r = 0.1$ (3, 4, 5, 6), $\alpha_{sc} = 14.1$ (1–6), $L = 10$ m (1, 3, 5), $L = 100$ m (2, 4, 6).

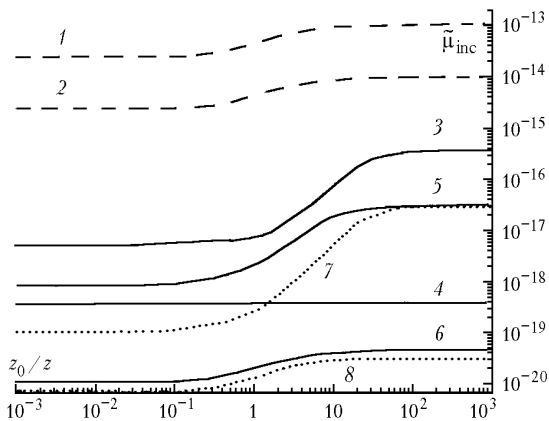


Fig. 5. Dependence of $\tilde{\mu}_{inc}$ on the position of a scattering layer when sensing a point-like object and at $a_{tr}/a_c = 0$, $R/F = 0$, $d/\lambda = 3$ (1, 2, 3, 4, 7, 8), $d/\lambda = 1$ (5, 6), $a_{tr}/a_r = 1$ (1, 2, 5, 6, 7, 8), $a_{tr}/a_r = 0.1$ (3, 4), $\alpha_{sc} = 1.41$ (1–8), $L = 10$ m (1, 3, 5, 7), $L = 100$ m (2, 4, 6, 8).

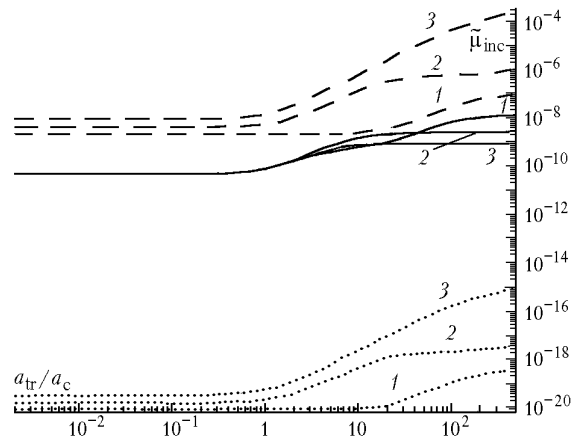


Fig. 6. Dependence of $\tilde{\mu}_{inc}$ on the initial length of spatial coherence of the transmitter when sensing specular (—), point-like (····), and diffuse (---) reflectors at $d/\lambda = 3$, $a_{tr}/a_r = 1$, $R/F = 0$, $\alpha_{sc} = 14.1$, $L = 100$ m, $R = 4100$ m, $z_0 = 100$ m (1), $z_0 = 2000$ m (2), and $z_0 = 3900$ m (3).

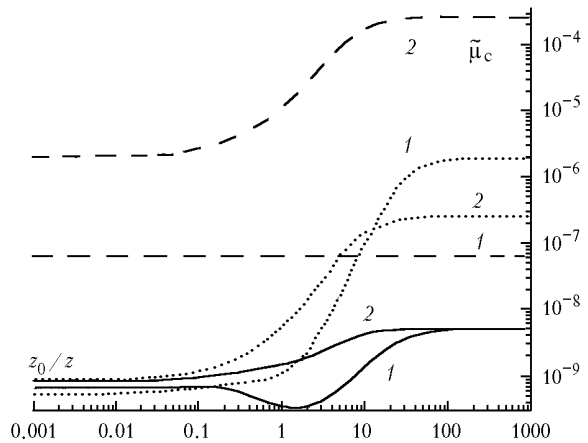


Fig. 7. Dependence of $\tilde{\mu}_c$ on the position of a scattering layer when sensing specular (—), point-like (····), and diffuse (---) reflectors at $\alpha_{sc} = 14.1$, $d/\lambda = 3$, $L = 10$ m, $a_{tr}/a_c = 0$, $R/F = 0$, $R = 4100$ m (1) and $R = 2100$ m (2).

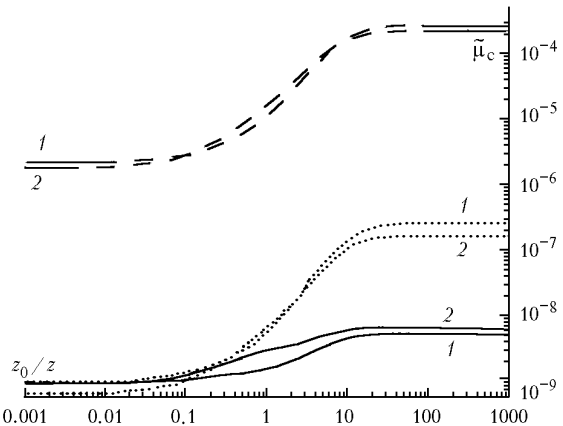


Fig. 8. Dependence of $\tilde{\mu}_c$ on the position of a scattering layer when sensing specular (—), point-like (····), and diffuse (---) reflectors at $\alpha_{sc} = 14.1$, $d/\lambda = 3$, $a_{tr}/a_c = 0$, $L = 100$ m, $R = 2100$ m, $R/F = 0$ (1) and $R/F = 1$ (2).

Figures 6 and 9 show the calculated results on μ_{inc} as a function of coherent properties of sounding radiation, as well as of scattering properties of the objects sounded. The calculations showed that regardless of the reflector type, the efficiency grows with the increasing ratio a_{tr}/a_c , because the radiation characteristics at the exit from the scattering layer only weakly depend on the coherent properties of the radiation at the layer entrance. The nonmonotonic character of the dependence $\mu_{\chi} = \mu_{\chi}(a_{\text{tr}}/a_c)$ is caused by the competition among the diffraction effects: increase of the coherence length as the beam propagates in free space and loss of the spatial coherence in the scattering layer. This phenomenon is qualitatively similar to the nonmonotonic character of the dependence of the spatial coherence length on the initial coherence length of a transmitter in the turbulent atmosphere.⁴

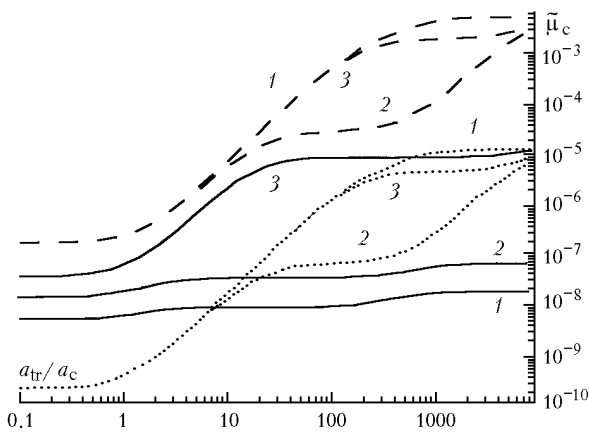


Fig. 9. Dependence of $\tilde{\mu}_c$ on the initial length of spatial coherence of transmitter when sensing specular (—), point-like (···) and diffuse (---) objects and at $d/\lambda = 3$, $a_{\text{tr}}/a_r = 1$, $R/F = 0$, $\alpha_{\text{sc}} = 14.1$, $L = 100$ m, $R = 4100$ m, $z_0 = 100$ m (1), $z_0 = 2000$ m (2), $z_0 = 3900$ m (3).

Conclusion

So, using the Huygens–Kirchhoff method and solving the equation of radiative transfer in the small-angle approximation, we have developed the engineering technique for estimating the influence of a localized scattering layer on the efficiency of operation of a lidar system with a direct and heterodyne detection of the return signal.

The comparison of the results obtained by this technique with those obtained both experimentally and

with the use of the diffusion version of the small-angle approximation showed that this technique allows obtaining results, which are in good qualitative agreement with the known ones.

It was found that the efficiency of operation through a localized scattering layer is lower for an incoherent lidar system than for a coherent one. This is connected with the influence of the backscattering noise on the efficiency of incoherent lidar systems.

It was found from this study that the efficiency of a lidar system depends mostly on the power extinction in the layer. As the optical density of the layer increases, diffraction effects, which are most pronounced when sensing specular reflectors, become more significant.

References

1. V.M. Orlov, I.V. Samokhvalov, G.M. Krekov, et al., *Signals and Noise in Lidar Sensing*, ed. by V.E. Zuev (Radio i Svyaz', Moscow, 1985), 264 pp.
2. V.M. Orlov, I.V. Samokhvalov, G.G. Matvienko, et al., *Elements of Light Scattering Theory and Optical Detection and Ranging*, ed. by V.M. Orlov (Nauka, Novosibirsk, 1982), 225 pp.
3. V.E. Zuev and M.V. Kabanov, *Optics of Atmospheric Aerosol* (Gidrometeoizdat, Leningrad, 1987), 254 pp.
4. V.A. Kovalev, *Visibility in the Atmosphere and Its Estimation* (Gidrometeoizdat, Leningrad, 1988), 215 pp.
5. I.N. Matveev, V.V. Protopopov, I.N. Troitskii, et al., *Laser Detection and Ranging*, ed. by N.D. Ustinov, (Mashinostroenie, Moscow, 1984), 272 pp.
6. P.A. Bakut, I.A. Bol'shakov, B.M. Gerasimov, et al., *Problems of Statistical Theory of Radio Detection and Ranging*, ed. by G.P. Tartakovskii (Sov. Radio, Moscow, 1963), Vol. 1, 424 pp.
7. V.V. Protopopov and N.D. Ustinov, *Laser Heterodyning* (Nauka, Moscow, 1985), 200 pp.
8. A. Ishimaru, *Wave Propagation and Scattering in Random Media*. Part 1. *Single Scattering and Transfer Theory* (Academic Press, New York, 1978).
9. A. Ishimaru, *Wave Propagation and Scattering in Random Media*. Part 2. *Multiple Scattering* (Academic Press, New York, 1978).
10. M.I. Abramowitz and I.M. Stegun, eds., *Handbook of Mathematical Functions* (U.S. Govt. Printing Office, Washington, 1972).
11. A.P. Ivanov, I.I. Kalinin, A.L. Skrelin, and I.D. Sherbaf, *Izv. Akad. Nauk SSSR, Ser. Fiz. Atmos. Okeana*, No. 8, 884–890 (1972).
12. E.P. Zege, A.P. Ivanov, and I.L. Katsev, *Image Transfer through Scattering Medium* (Nauka i Tekhnika, Moscow, 1985), 327 pp.
13. M. Born and E. Wolf, *Principles of Optics* (Pergamon Press, New York, 1959).